AIAA JOURNAL
Vol. 41, No. 11, November 2003

Laser-Induced Breakdown Spectroscopy of Hydrocarbon Flame and Rocket Engine Simulator Plume

Virendra N. Rai,* Jadish P. Singh,† Chris Winstead,‡ Fang-Yu Yueh,§ and Robert L. Cook¶
Mississippi State University, Starkville, Mississippi 39759-7704

Laser-induced breakdown spectroscopy (LIBS) of metal-seeded aerosols and a hydrocarbon flame were studied to determine the proper experimental condition for rocket motor application. LIBS and atomic emission spectroscopy (AES) were also performed in the rocket motor simulator to evaluate both technologies for the health monitoring of the rocket engine. The LIBS signal of the seeded element goes down drastically in the presence of the flame in comparison to the signal obtained from the aerosols of the elements. Similarly the LIBS signal of the trace elements was very weak in the luminous flame and the simulator plume in comparison to the measurement outside it. The intensity of the LIBS signal from the trace elements present in the plume/flame was found to be dependent on the process of seeding, the transition probability, and the decay time of the background emission. Ultimately LIBS was found to be more sensitive than AES in detecting the trace elements in the simulator plume. This study establishes LIBS as an improved health-monitoring system over AES for the plume studied.

Introduction

THE development of the next generation of rocket motors using hydrocarbon fuels requires a reliable system for motor health monitoring during testing.[1–4] Robust detection and characterization of metallic species in the exhaust plume of hydrocarbon-fueled rocket motor would be an important development for this purpose. The presence of metallic species in the plume indicates wear and/or corrosion of metal inside the rocket motor. Any information obtained on the motor wear during its operation is very useful to allow the possibility of engine shutting down before catastrophic failure. It has been observed that a catastrophic engine failure was generally preceded by intense optical emission, which resulted from erosion of metal from the engine parts. This is because the high temperature of the rocket plume (>2000 K) partially vaporizes and atomizes the metal species, leading to the atomic emission in the near ultraviolet and visible spectral range (300–760 nm). One traditional method to monitor the engine plume during a test is atomic emission spectroscopy (AES) in the near ultraviolet and visible spectral region,[1–3] particularly for hydrogen-fueled motor. However, a hydrocarbon-fueled motor contains various species in its plume in the form of atomic carbon C_2^+ and other carbon free radicals that increase the background emission from the plume significantly more than the main OH band, generally observed in oxygen- and hydrogen-fueled engines. Even the scattering from the unburned carbon produces a strong background, increasing the opacity of the plume, another disadvantage for the atomic emission spectroscopic technique in detecting the presence of metal corrosion and engine wear in a hydrocarbon-fueled rocket engine. This indicates the need for a sensitive technique to detect the presence of trace elements in hydrocarbon plumes.

Laser-induced breakdown spectroscopy (LIBS) is a laser-based diagnostics technique that has proven to be effective for measuring the concentration of elements in various types of test media including solids, liquids, and gases.[5–12] The laser-induced breakdown plasma consists of electrons and ions, as well as neutral particles. The optical signals from neutral and ionized atoms are collected to obtain the emission spectrum using a proper detection system. The analysis of the LIBS spectrum provides information about the elemental concentration in the test medium. The LIBS technique has several notable advantages over other analytical techniques. It uses a very small sample without any special preparation and can perform real-time analysis. LIBS also can operate in harsh and difficult environmental conditions. The real-time continuous monitoring capability of LIBS has been demonstrated in production control and quality assurance in the steel industry[13] and off gas from combustion facilities.[14–16] LIBS has also been applied to a harsh, turbulent and highly luminescent coal-fired magnetohydrodynamic gas stream.[17] It can provide an alternate technique that offers better elemental sensitivity and the ability to probe a hydrocarbon flame or rocket engine plume at different locations.[4,18]

In the present paper, we describe the LIBS of a metal-seeded hydrocarbon flame to establish the proper experimental conditions for recording the LIBS of a rocket engine simulator plume. LIBS and AES was performed in the rocket engine simulator to compare the sensitivity of both techniques for the health monitoring of the rocket engines. The OH emission spectrum of the plume was also used to estimate the temperature of the plume. Finally, different methods of metal seeding in the plume are discussed.

Instrumentation

Experiments were conducted on a metal-seeded hydrocarbon flame and hybrid rocket engine simulator using a LIBS system and AES to investigate the feasibility using LIBS as a rocket engine health monitor. A brief introduction to all of the components of the experimental setup is presented.

Hydrocarbon Flame

A schematic diagram of the burner for generating the hydrocarbon flame is shown in Fig. 1. The burner is made of brass and has metallic mesh at one end that helps in sustaining the flame. The lower end has three stainless steel tubes attached as inlets. These tubes serve for injecting hydrocarbon fuel, air, and the dry aerosols of sample elements that are mixed before reaching in the reaction zone of the flame and the air. The proper regulation of the ratio of fuel-to-oxygen

Received 13 August 2002; revision received 10 April 2003; accepted for publication 1 May 2003.

*Visiting Scientist, Diagnostic Instrumentation and Analysis Laboratory, 205 Research Boulevard; currently on leave, Scientist, Laser Plasma Division, Centre for Advanced Technology, Indore 452 013, India.

†Research Professor, Diagnostic Instrumentation and Analysis Laboratory, 205 Research Boulevard; singh@dial.msstate.edu.

‡Associate Research Professor, Diagnostic Instrumentation and Analysis Laboratory; currently Associate Professor, Department of Physics, University of Southern Mississippi, Hattiesburg, MS 39406-5046.

§Research Scientist I, Diagnostic Instrumentation and Analysis Laboratory, 205 Research Boulevard.

¶Director, Center for Advanced Energy Conversion, 205 Research Boulevard.

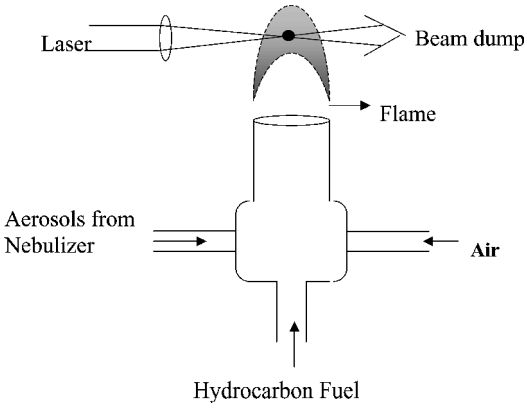

Fig. 1 Schematic diagram of burner for generating hydrocarbon flame.

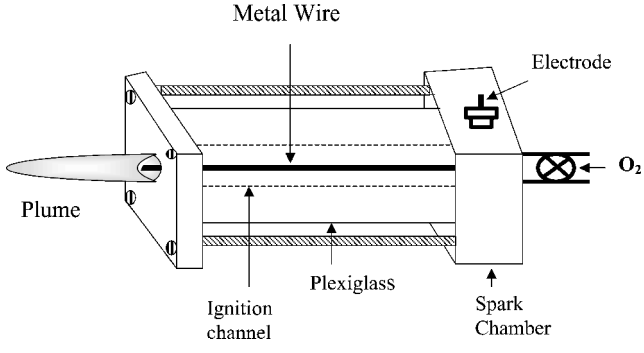

Fig. 2 Schematic diagram of hybrid rocket motor simulator.

(air) determines the stability of the flame. The flames used here were not turbulent during the experiment. The laser spark for LIBS was generated at various positions in the flame. The location of spark was shifted from the lower blue to yellow luminous zone of the flame to get the spatial information about the LIBS signal.

Rocket Engine Simulator

The hybrid rocket engine simulator (Fig. 2), provided by NASA Stennis Space Center, uses a solid cylindrical plexiglass rod as the fuel. This cylindrical plexiglass rod has an axial central hole that connects to a small stainless steel chamber, housing an electrode and the inlet for the introduction of oxygen gas. As Fig. 2 shows, the initial spark chamber and oxygen inlet lie on one side, whereas the exit nozzle for plume lies on the other side of the plexiglass rod. Steel wool was inserted into the spark chamber to start the initial combustion in the presence of oxygen flow. The combustion was started in the chamber using an electric current from a 12-V battery between the electrode and the conducting body of the spark chamber, with the steel wool as a conductor. The initial spark started ignition in the chamber, which propagated through the central axial hole of plexiglass rod toward the exit channel. An adequate flow of oxygen was maintained to ensure proper burning of the plexiglass fuel. The high-temperature combustion gas, exiting from the nozzle (diameter ~4 mm), produces a high-speed luminous plume of ~5–8 cm in length. It is necessary to inject the seed metal into the plume to study the presence of metallic content in the rocket motor simulator plume. Various metal doping methods were tested. In these initial efforts, a metallic wire was placed downstream the nozzle but in contact with the motor simulator plume. In another method, a metal wire was inserted through the ignition channel from the spark chamber to the exit nozzle through the axis of the plexiglass rod. It was found that the presence of the seed metal wire in the ignition chamber provided better results. This is because the metal is vaporized along the axis of the simulator due to the high temperature of the gas and exits with the exhaust gases through the nozzle. Copper and stainless-steel wires ($\phi \sim 1$ mm) were used as the seeding materials during the present experiment.

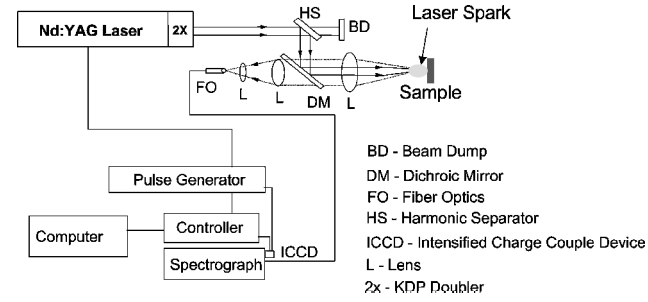

Fig. 3 Experimental system for recording LIBS of flame and rocket motor simulator plume. KDP, microhardness dihydrogen phosphate.

Experimental Setup

The schematic of the LIBS experimental setup used during this experiment is shown in Fig. 3. A Q-switched frequency-doubled Nd:YAG laser (Continuum Surelite III) that delivers energy of ~300-mJ pulse at a wavelength of 532 nm with repetition rate of 10 Hz and pulse width of 3–5 ns was used to generate a spark in the hydrocarbon flame (Fig. 1) and the rocket motor simulator plume (Fig. 2). The laser beam was reflected at a harmonic separator to remove its fundamental infrared component. The 532-nm beam was then reflected to the probe lens through a dichroic mirror, which reflects 532 nm but transmits other wavelengths. The laser was focused in the flame and in the rocket engine simulator plume using an ultraviolet grade quartz lens of 10-cm focal length to produce a breakdown spark. The same focusing lens was used to collect and collimate the emission from the breakdown plasma. The LIBS signal was transmitted through the dichroic mirror and coupled to the fiber optic bundle with additional two lenses. The bundle was formed with 80 single fibers. The core diameter of a single fiber was 0.1 mm, and the numerical aperture of the fiber bundle was 0.16. The configurations of the two ends of the bundle were round and rectangular, respectively. The round end was used as an entrance to accept the LIBS signal, and the rectangular end was used as an exit to couple the signal to an optical spectrograph. The spectrograph (Instruments SA, Inc., Model HR 460) was equipped with a 1200-l/mm diffraction grating of dimension 75 ×75 mm. A 1024 × 256 elements intensified charge-coupled device (ICCD) detector (Princeton Instrument) with a pixel width 0.022 mm was mounted at the exit of the spectrograph to record the spectrum. The spectral region monitored by the detector was ~30 nm wide with a resolution of ~0.15 nm with the 1200-l/mm grating. The detector worked in the gated mode and was synchronized to the laser Q switch. To maximize the signal over noise, a gate pulse delay of 30 μs and width of 10 μs was used in most of the work unless otherwise stated. Data acquisition and analysis were performed using a personal computer. The laser was focused at various locations of the flame and plume to record the LIBS spectra at different spatial locations. In the cases of the aerosols and the flame experiments, signals from 100 laser pulses were accumulated to obtain one spectrum. Finally 10 such spectra were averaged to get one data point. In the case of the rocket engine simulator plume measurement, to obtain time-resolved data in short operating time of engine simulator (~20 s), five laser pulses were averaged to form one spectrum.

The study of emission from the luminous plume can also provide important information about the content and condition of the plasma plume. A standard AES system was used for this purpose during the motor simulator test. Briefly, a lens was used to form 1:1 image of the plume onto an optical fiber. The position of the fiber could be moved in the image to allow for the acquisition of spectra from different regions of the plume. The light was collected on one end of a 1-mm-diam optical fiber, which transmits the emission to the input of a spectrometer. The type of fiber selected was optimized for ultraviolet light transmission. Light collected by the fiber was routed to a 0.5-m Acton spectrometer (Acton Research Co.), equipped with a

256 × 1024 pixel charge-coupled device (CCD) detector. A manual shutter mounted at the entrance slit to the spectrometer provided exposure control for the CCD detector. A 2400-line/mm grating was used in the collection of all of the atomic emission spectra.

Results and Discussion

LIBS of Aerosols

The best operating parameters for recording the LIBS spectrum with a good signal-to-noise ratio (S/N) and signal-to-background ratio (S/B) depend mainly on the laser energy and the emission properties (spectral region) of the sample along with its surrounding conditions. Therefore, it was important to find the best operating conditions for the measurement of aerosols and a metal-seeded hydrocarbon flame to approximate optimum conditions for recording of LIBS of the rocket engine simulator plume. Solutions of Fe, Cr, and Ni with concentrations of 200, 20, and 500 μg/ml, respectively, were prepared for generating aerosols and seeding the hydrocarbon flame. Mixture solutions were pumped to a nebulizer through a peristaltic pump to generate and inject dry aerosols in the burner through one of the channels as shown in Fig. 1. The LIBS spectrum of the mixed aerosols (Fe, Cr, and Ni) was recorded first in the absence of the flame and is shown in Fig. 4. The spectrometer was set at a central wavelength of 370 nm to capture emission lines from each of the injected elements. The LIBS spectra show various emission lines corresponding to all three elements, present in the form of aerosols. The optimum S/B ratio was found for 30-μs gate delay and 10-μs gate width set for the ICCD detector. Note that the iron and nickel line intensities were comparatively better in comparison to chromium. This is because of the low (20-μg/ml) concentration of Cr in comparison to iron (200 μg/ml) and nickel (500 μg/ml). The chromium lines intensities are clearly visible in spite of the low chromium concentration, indicative that chromium has a larger transition probability than iron and nickel. The presence of the CN band is also observed in this spectrum. CN is produced in the laser spark in air due to the reaction of C and N atoms.[11] The small amount of dust and CO_2 present in air can contribute toward carbon. However, the intensity of CN band here is much weaker than in the LIBS spectrum of hydrocarbon flame, where a source of carbon is present.

To study the effect of airflow (air is injected in the nebulizer to extract the dry aerosols out of it) in the nebulizer on the S/B and S/N of LIBS spectra of the mixtures of iron, nickel, and chromium aerosols were recorded for three different rates of airflow in the nebulizer. The rate of airflow was varied from 200 to 800 ml/min, which corresponds to air speed ~70–280 cm/s. Figure 5 shows that the intensities of all of the lines from iron, chromium, and nickel increase with an increase in the rate of airflow. This indicates that the increase in the rate of airflow ultimately increases the effective number of atoms (dragged with airflow) in the spark, which finally aids in increasing the LIBS intensity. It was found that the efficiency of the nebulizer changes with the gas flow rate. The effect of comparatively higher flow rates of air on the LIBS intensity has already been reported.[4] Previous experiments were performed on a small-scale combustion test stand, which is a low flow rate, bench-scale combustion (50-lb/h air maximum) train. Initial studies were performed to study the effect of gas flow rate on the LIBS calibration with the help of a calibrated nebulizer to inject metal aerosols into the preheated gas. In this experiment, aerosols were injected in the hot airflow at a constant speed. The hot airflow in the combustion test stand dilutes the concentration of dry aerosols (analyte atoms). In this case, a linear relation was found between the LIBS signal and the inverse of gas flow rate.

During this experiment, various concentrations of liquid solution were injected in the nebulizer to produce dry aerosols. The airflow in this case was kept constant at ~280 cm/s. The effect of solution concentration on the LIBS of aerosols in air is reflected in the calibration curve for iron shown in Fig. 6. The calibration curve of Cr was found to be similar. The concentration of iron in the mixture was varied from 50 to 200 μg/ml, whereas it was 5–20 μg/ml for chromium. The LIBS signal increases with an increase in the concentration of iron and was due to an increase in the ablated iron atom in the laser plasma. The calibration curve for both the elements was found to be linear. A comparatively higher signal obtained from chromium even at its lower concentration is due to its higher transition probability as discussed earlier. This calibration curve clearly indicates that the system is quite capable of detecting a trace of the elements present in the form of aerosols. The limits of detection for the elements are particularly dependent on the rate of flow, the volume of the system to which aerosols are being injected, and the location of the spark formation in the gaseous environment.[4,18]

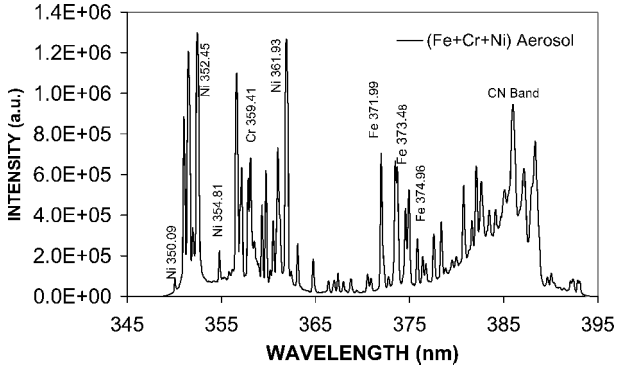

Fig. 4 LIBS spectrum of aerosols of iron, chromium and nickel (laser energy ~100 mJ and gate delay/gate width ~30/10 μs).

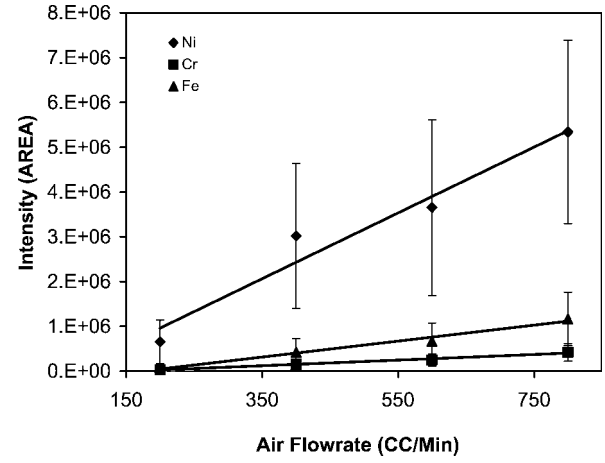

Fig. 5 Variation in LIBS intensity of aerosols of iron, chromium and nickel with the rate of airflow in nebulizer (laser energy ~100 mJ and gate delay/gate width ~30/10 μs).

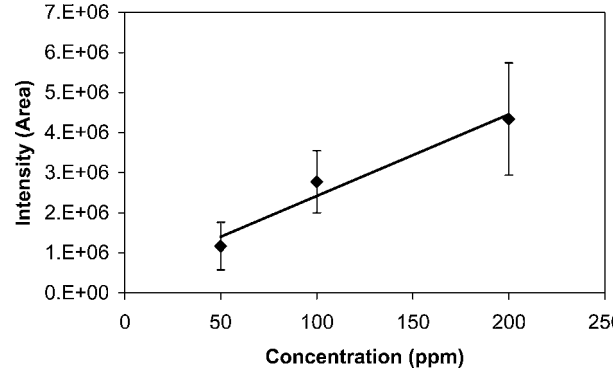

Fig. 6 Variation in the intensity of LIBS from iron aerosols in air with the concentration of iron solution (laser energy ~100 mJ and gate delay/gate width ~30/10 μs).

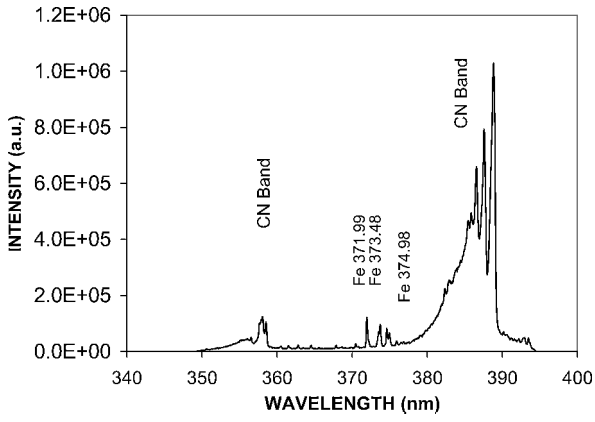

Fig. 7 LIBS spectra of hydrocarbon flame seeded with iron (laser energy ~155 mJ and gate delay/gate width ~40/10 μs).

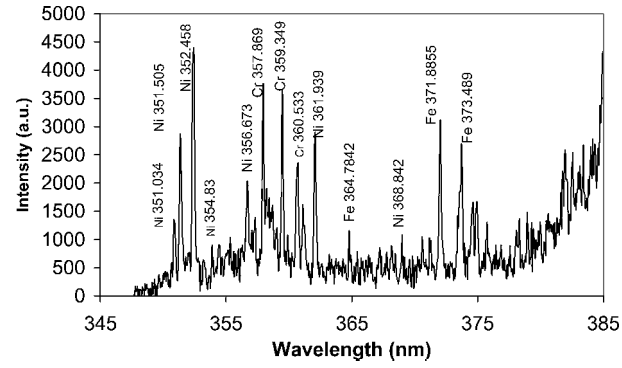

Fig. 8 LIBS spectra of hydrocarbon flame seeded with mixture of iron, chromium, and nickel (laser energy ~155 mJ and gate delay/ gate width ~80/10 μs).

LIBS of Metal-Seeded Hydrocarbon Flame

The burner used for generating the hydrocarbon flame has a diameter of 1.5 cm and premixes the liquid hydrocarbon fuel (kerosene) with the airflow. The flow rates of the air and liquid hydrocarbon fuel were adjusted to obtain a stable, turbulence-free flame. The aerosol mixtures of iron, chromium, and nickel were injected into the flame through a separate channel to the burner. The seed elements were mixed with the fuel before ignition. The laser was focused initially in the luminous zone of the flame to generate a spark for recording the LIBS spectra. Various flame conditions were tested to optimize LIBS measurements. Figure 7 shows the LIBS spectra of the iron-seeded flame in the spectral region, ranging from 350 to 395 nm. Very strong CN emission bands were observed around 359 and 385 nm, which is expected as discussed earlier. It is understood that the use of an oxidizer that does not contain nitrogen will dramatically reduce the intensity of the CN band. These results are similar to previous report.[18] Because the flame conditions vary at different distances from the burner head, variations were observed in emission from the iron, chromium, and nickel. The intensity of the line emission varies as a function of distance from the burner head. Note that the LIBS signal from the elements injected into the flame is stronger in the blue region of the flame in comparison to the yellow luminous region. This may be due to two reasons. 1) The blue zone of the flame is close to the burner exit nozzle, where density of the analyte elements will be more. This concentration decreases as the aerosols diffuse away from the nozzle. 2) The background signal was less in the blue region than in the yellow luminous zone of the flame. A comparison of the LIBS signal from the elemental aerosols in the air (Fig. 4) and in the flame (Fig. 7) shows that the LIBS signal of the aerosols are stronger in air. This is either due to an increase in the background emission from the luminous flame, or due to the depletion of elemental density in the flame as a result of thermal and chemical effects.

Temporal evolution of the LIBS of the metal-seeded flame also provides important information. The LIBS spectrum of the hydrocarbon flame with metal seeds (Fe, Cr, and Ni) recorded at a gate delay of 40 μs from the laser firing showed the presence of line emissions from Cr and Ni superimposed on the CN band near 359 nm. No iron emission lines were observable in this spectrum. In fact, the S/B ratio was very small. The LIBS spectrum of the seeded flame recorded at 50-μs gate delay showed the onset of iron lines. In this case, S/B ratio increased in such a way that the emission lines from iron along with chromium and nickel were also observable. However S/B ratio was still very low. Finally all of the emission lines from Fe, Cr, and Ni became very clear at 80-μs gate delay (Fig. 8) due to the drastic decrease in the background emission of the spark, which makes the S/B ratio comparatively high. The emission lines from all of the elements were very clear. The observation of only Cr and Ni emission lines at 40-μs gate delay in comparison to iron line seems to be due to the higher concentration of nickel (500 ppm) and the larger transition probability of Cr (10 ppm) than iron (100 ppm)

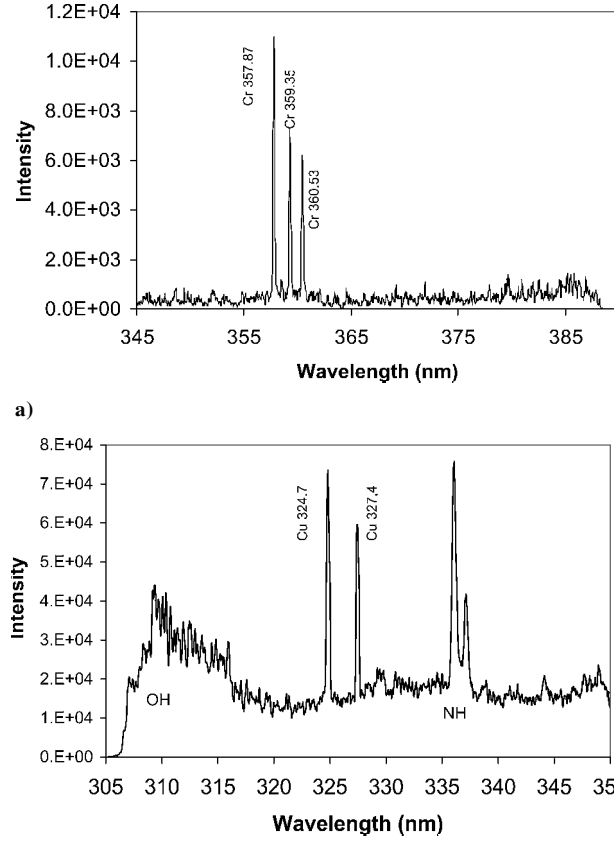

Fig. 9 LIBS spectrum of rocket engine plume (laser energy ~280 mJ and gate delay and gate width 30/10 μs): a) with stainless-steel seed and b) with copper seed.

(Refs. 19 and 20). Also a comparatively higher optimum gate time (~80 μs) was observed for Fe than for Cr and Ni. It is clear from this study that, to observe the line emission from the luminous flame, one has to record the (LIBS) spectrum after optimizing the gate time delay to increase the S/B ratio. The optimum time delay varies from element to element. The optimum time delay for most of the elements of interest in the desired experimental condition will need to be carefully evaluated.

Study of Rocket Engine Simulator Plume

LIBS Study of Simulator Plume

The LIBS spectrum of the engine simulator plume was recorded with a 316L stainless-steel wire of 1.76-mm diam inserted into the ignition chamber to generate the seed vapor in the plume. The laser was focused approximately 7.5 cm from the exit of the nozzle. Figure 9a shows the presence of strong atomic emission lines of

chromium in the LIBS spectrum of plume. The chromium emission lines are observed in the spectrum because stainless steel 316L contains ~17% Cr. LIBS spectra of the plume indicated the presence of a significant amount of Cr in the plume, whereas no iron lines were observed in the spectra at this location. This behavior is likely due to the low concentrations of iron near the exit channel where the plume speed is very high and the possibility that the gate delay time of 30 μs may not be sufficient for the observation of iron emission lines as discussed earlier. The observation of chromium lines in spite of its lower concentration than iron in stainless steel is likely due to a high transition probability. The limit of detection of Cr has already been reported in the hot airflow as 6 μg/actual cm (Ref. 11). These observations are similar to those for LIBS spectra recorded from the hydrocarbon flame seeded by the mixture of Fe, Cr, and Ni. As discussed earlier, the spectrum recorded at 40-μs gate delay in flame showed that the Cr lines were present, whereas Fe lines were absent, even in the condition when the iron concentration was quite high in comparison to the chromium. However, emission lines from the iron became prominent when the spectrum was recorded at a gate time delay of 80 μs (Fig. 8). This clearly explains the observation of only chromium in the simulator plume (Fig. 9a). A trace of iron was observed in the LIBS spectra of the plume, when the spectrum was recorded at higher gate delay. The observed iron signal was very weak, which might be due to the dilution of the concentration of iron in the high speed of plume. (Note the earlier discussion that the LIBS is inversely proportional to the speed of hot gases.)

The LIBS spectra of the plume ranging from 305 to 350 nm were also recorded for copper doping (Fig. 9b). The spectrum recorded in this spectral region shows two strong emission lines from atomic copper along with the strong emissions from OH and NH radical bands. Two strong copper line emissions from the plume were found when a copper wire was placed in contact with the plume, just downstream of the exit nozzle. The observation of a strong OH band was found useful in estimating the temperature of the simulator plume. For this purpose, the emission spectrum of the plume was recorded as discussed in the following text. However, with this seeding method, we could only detect copper for a fraction of second because it was vaporized very rapidly. Because the copper spectrum was observed for a very short time in the initial seeding method, we placed the copper wire inside the ignition chamber as already discussed and shown in Fig. 2. The LIBS spectra of the plume were recorded at different spatial locations from the exit nozzle.

Figure 10 shows the temporal evolution of the stronger copper line emission, obtained from the LIBS spectra recorded at different

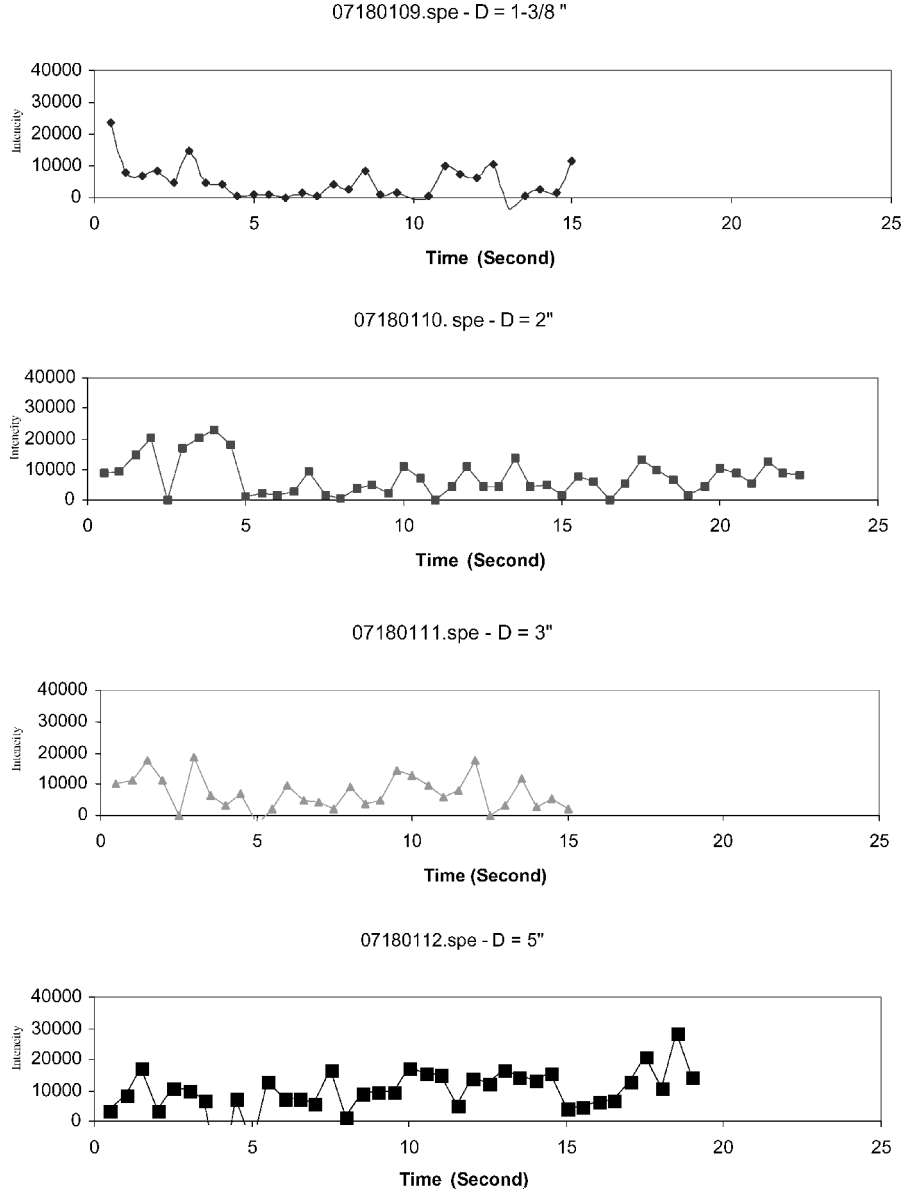

Fig. 10 Temporal and spatial variation of LIBS signal in rocket engine simulator plume, where *D* is the distance between the laser induced spark and the exit nozzle of the plume (laser energy ~280 mJ and gate delay/gate width ~30/10 μs).

spatial locations of the plume (3.5, 5, 7.5, and 12 cm from the exit nozzle) for four different firing. In this experiment, copper wire was used as the seed sample inside the ignition chamber. The presence of copper in the plume was detected strongly in the LIBS spectra, recorded near the nozzle exit during the initial fractions of a seconds as the plume started to build. Note that the LIBS signal decreases when the plume attains its full length (>5 cm), high temperature, and high speed. It was found that, as the measurement point moved away from the plume exit channel, the copper lines were detected all through the presence of plume. The background emission from the plume was also decreased as the measurement location was shifted away from the luminous zone. The stronger signal, away from the exit nozzle, seems to be due to the better mixing of the metal vapor and exhaust gases in the plume. The plume has a lower speed and lower gas temperature at this location as compared to the region near the exit nozzle. The data from these preliminary tests show that the measurements made away from the luminous part of the plume can provide a strong indicator for the presence of trace elements in the rocket engine plume, perhaps an indication toward excessive wear in the system.

Standard Emission Spectroscopy of Simulator Plume

The estimation of the temperature in the rocket engine plume is possible by quantitatively comparing the results of experiments with those from computer simulation. The temperature information is necessary to relate the population of a particular rotational and vibrational level, measured spectroscopically. Normally a temperature profile is used as input for computer simulation, which is compared with the experimental observation. The demand for the accuracy of the temperature measurements is rather high because of the strong nonlinear dependence of the reaction rate on the temperature. There are many methods to measure the gas temperature in hydrocarbon flames,[21–23] including both intrusive probe measurements and nonintrusive light scattering techniques. One widespread method of temperature measurement for flames is to determine the rotational temperature of a molecule present in the flame. One of the best targets for such measurements is the OH radical. The spectrum of the OH radical has proved to be a very useful thermometer in the flames.[21] These radicals remain in all parts of hydrocarbon and hydrogen flames and have large rotational constants, which makes such measurements suitable. An emission spectrum from the rocket engine plume that contains the OH radical emission can be a good technique for estimating the plume temperature. However, the accuracy of temperature measurements depends greatly on the dynamic range and the linearity of the signal provided by the technique used.

Emission spectra from the luminous plume of the rocket engine were also recorded for comparison with the LIBS spectra, as well as to estimate the plume temperature. During this experiment, copper wire was used as the seeding element near the exit nozzle of the simulator. Figure 11 shows the emission spectrum of the plume, which was recorded nearly ~3 s after ignition of the motor. The emission of the OH molecular band around 315 nm and two copper emission lines are evident. These observations are similar to those noted for the LIBS spectrum. However, a simple comparison of both the spectra demonstrates the enhanced Cu signal obtained with LIBS vs standard emission spectroscopy.

The temporal evolution of the copper emission was also obtained by plotting the integrated signal of the line emission as a function of time. Figure 12 shows that the copper signal can be seen using standard emission spectroscopy for nearly ~10 s before returning to the background intensity level. The engine has started at approximately t = 0 s. The comparison of temporal evolution of LIBS (Fig. 10) with optical emission data (Fig. 12) shows that the copper optical emission remains detectable during the initial period only, whereas the LIBS signal of copper from the plume lasts for the duration of motor firing (~20 s) but with a comparatively lower intensity of the signal.

The experimental spectrum, revealing the entire structure of this OH radical band in the emission from plume, is presented in Fig. 13a. The temperature of the plume was estimated using a simulation

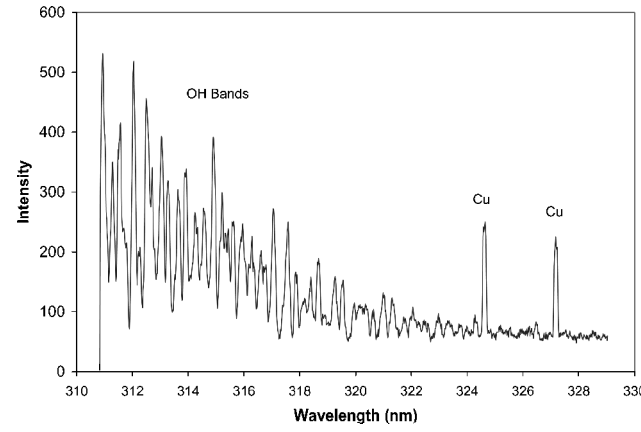

Fig. 11 Atomic emission spectrum of copper-seeded rocket simulator plume.

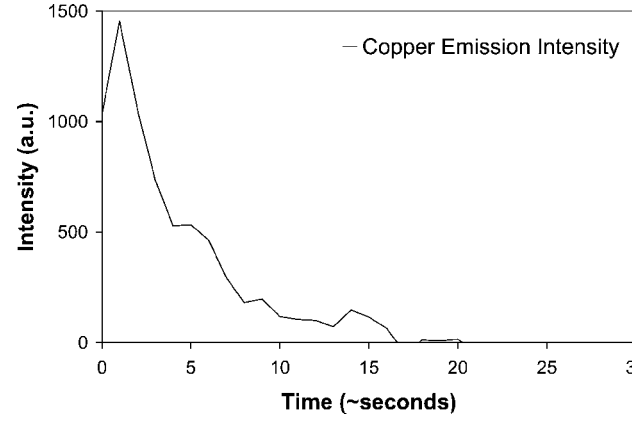

Fig. 12 Temporal evolution of copper line emission intensity from the simulator plume.

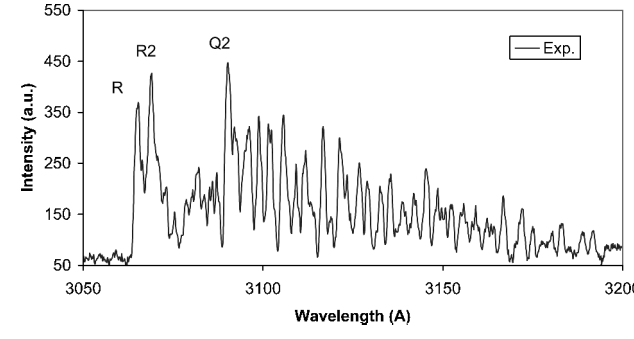

Fig. 13a Emission spectrum of OH radical, recorded from the simulator plume.

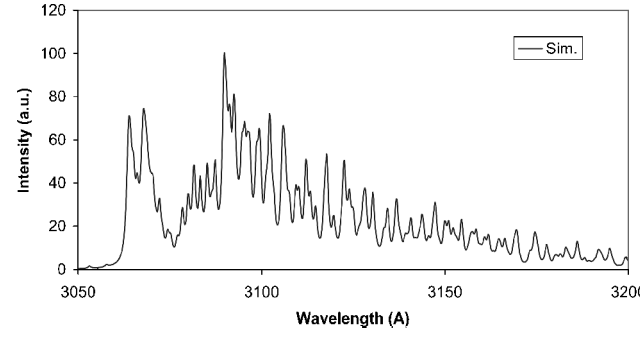

Fig. 13b Computer simulated spectrum of OH radical at 3300-K plume temperature.

program. The LIFBASE database and spectral simulation program[24] was used. The LIFBASE program provides Einstein emission and absorption coefficients, radiative lifetimes, transition probabilities, frequencies and Honl–London factors for many bands of OH (A–X), OD (A–X), CH (A–X, B–X, and C–X), NO (A–X, and D–X), etc. This spectral simulation program has been used to simulate the spectrum of the OH band, observed as in the standard emission spectrum. The detailed rotational structure of the OH band emission is evident in Fig. 13a. This structure is due to the emission from the A–X electronic transition and is composed of emission from the two lowest vibrational levels of the A state to the two lowest vibrational levels of ground state. The three largest peaks, toward the lower wavelength end of the scale, are R_1, R_2 and Q_2 rotational structure band heads as indicated in Fig. 13a. Below temperatures of approximately 2800 K, simulation indicates that the R_1 band head yields a larger intensity signal than the nearby R_2 structure. These features reach similar intensities near 2800 K, and the R_2 intensity exceeds that of the R_1 structure at higher temperatures. When the simulated spectrum (Fig. 13b) is compared with the experimentally obtained spectrum of Fig. 13a, it is evident that the OH temperature in the rocket plume exceeds 2800 K. Estimates, obtained using these simulations, suggest a temperature of approximately 3300 ± 800 K. More advanced comparisons between the simulated and experimental spectra can be used to provide more accurate temperature data. The OH emission spectrum presented here is a line-of-sight average. However, accuracy in the data can be improved by recording OH emission spectra at various lateral positions in the plume for subsequent conversion to radial profiles by using Abel inversion.

Conclusions

In summary, the LIBS study of aerosols and metal-seeded plumes indicates that the LIBS signal is lowest in the luminous flame region. The temporal evolution of the LIBS emission from the trace elements (Fe, Cr, and Ni) in the flame indicates that the S/B ratio increases at comparatively longer gate delay times. This is due to the fast decay of background plasma emission from the spark relative to the line emission from the trace elements present in the plume. Therefore, some elements such as iron are not observable at lower gate delay even at significant concentrations in the flame. The gas flow rate of the sample also affects the LIBS signal significantly. The LIBS signal decreases at higher airflow rate due to a decrease in the mass/volume of the analyte at experimental location, which is a dilution effect.

The LIBS spectra of the rocket engine simulator plume, seeded with stainless steel and copper, indicate that the signal is stronger when the LIBS spark is formed out of the luminous zone away from the exit nozzle. Better mixing of the exhaust gas and seeded elements was noted away from the exit nozzle. Strong background emission results in a small S/B ratio in the flame itself. Two techniques were employed for seeding the elements in the simulator plume. Of theses two, placing the metallic wire inside the ignition chamber was found to be the best. A better solution to seed the elements into the ignition chamber is one that can provide improved mixing and symmetrical injection of seeded elements in the plume.

Standard emission spectroscopy of the simulator plume provided a line-of-sight estimate of the gas temperature. However, strong background emission from the plume limits the accurate measurement of metals at trace levels. This problem is evident in the spectra obtained using the standard emission during this test. A simple comparison indicates that the LIBS technique has several advantages as compared with standard emission methods. In LIBS, a high-energy, pulsed laser beam is used to produce atomic emission at the focal volume, providing a time and spatially resolved measurement. Gated detection with an ICCD detector also discriminates against continuous background emission, which improves detection limits for the metallic species. Comparison of the spectra obtained from LIBS and emission shows that the LIBS spectra have higher S/N and S/B ratios (nearly two times with 10–15% variation).

The measurement of LIBS in the plume of a hybrid rocket engine simulator suggests that LIBS may have the capability to be a rocket engine health monitor to detect the trace metals, originating from the engine wear. To develop LIBS as a rocket engine health monitor, future work must include the investigation of methods for quantitative metal seeding and optimization of the experimental setup for reducing spectral interferences and to achieve a better LIBS sensitivity for trace element measurement.

Acknowledgments

This work is supported by Subcontract 00-07-010 between the University of Mississippi and Mississippi State University under NASA Cooperative Agreement NCC5-405. The assistance of William St. Cyr of NASA Stennis Space Center (SSC) and Gregory P. McVay and Lester Langford of Lockheed Martin Stennis operations during the measurement at NASA/SSC is gratefully acknowledged. All simulations were carried out using free software (version 1.70) provided by Jorge Luque of Stanford Research International.

References

[1]Gardner, D. G., Bircher, F. E., Tejwani, G. D., and Van Dyke, D. B., "A Plume Diagnostics Based Engine Diagnostics System for the SSME," AIAA Paper 90-2235, July 1990.

[2]Tejwani, G. D., Van Dyke, D. B., Bircher, F. E., Gardner, D. G., and Chenevert, D. J., "Emission Spectra of Selected SSME Elements and Materials," NASA RP 1286, 1992.

[3]Tejwani, G. D., Bircher, F. E., Van Dyke, D. V., McVay, G. P., Stewart, C. D., and Langford, L. A., "Space-Shuttle Main Engine Exhast-Plume Spectroscopy," *Spectroscopy*, Vol. 11, 1996, pp. 31–45.

[4]Loge, G. W., Singh, J. P., Yueh, F. Y., and Zhang, H., "Hydrocarbon Fueled Rocket Engine Health Monitoring by Laser Induced Breakdown Spectroscopy," Final Rept., Contract NASA 13-99002, Small Business Technology Transfer Phase 1, 27 Oct. 1999.

[5]Cremers, D. A., and Radziemski, L. J., "Laser Plasma for Chemical Analysis," *Laser Spectroscopy and Its Applications*, edited by L. J., Radziemski, R. W. Solarz and J. A. Paisner, Dekker, New York, 1987, Chap. 5, pp. 351–415.

[6]Thiem, T. L., Lee, Y. I., and Sneddon, J., "Laser in Atomic Spectroscopy: Selected Application," *Microchemical Journal*, Vol. 45, 1992, pp. 1–35.

[7]Rusak, D. A., Castle, B. C., Smith, B. W., and Winefordner, J. D., "Fundamentals and Applications of Laser Induced Breakdown Spectroscopy," *Critical Reviews in Analytical Chemistry*, Vol. 27, No. 4, 1997, pp. 257–290.

[8]Neuhauser, R. E., Panne, U., and Niessner, R., "Laser-Induced Plasma Spectroscopy (LIPS): A Versatile Tool for Monitoring Heavy Metal Aerosols," *Analytica Chimica Acta*, Vol. 392, 1999, pp. 47–54.

[9]Ciucci, A., Palleschi, V., Rastelli, S., Barbini, R., Colao, F., Fantoni, R., Palucci, A., and Ribezzo, S., "Trace Pollutants Analysis in a Soil by a Time-Resolved Laser-Induced Breakdown Spectroscopy Technique," *Applied Physics B*, Vol. 63, 1996, pp. 185–190.

[10]Knopp, R., Scherbaum, F. J., and Kim, J. I., "Laser-Induced Breakdown Spectroscopy (LIBS) as an Analytical Tool for the Detection of Metal Ion in Aqueous Solutions," *Fresenius' Journal of Analytical Chemistry*, Vol. 72, 1996, pp. 4731–4736.

[11]Song, K., Lee, Y. I., and Sneddon, J., "Application of Laser-Induced Breakdown Spectroscopy," *Applied Spectroscopy Review*, Vol. 32, No. 3, 1997, pp. 183–235.

[12]Yueh, F. Y., Singh, J. P., and Zhang, H., "Laser Induced Breakdown Spectroscopy: Elemental Analysis," *Encyclopedia of Analytical Chemistry*, Vol. 3, Wiley, New York, 2000, pp. 2065–2087.

[13]Noll, R., Bette, H., Brysch, A., Krausharr, M., Monch, I., Peter, L., and Sturm, V., "Laser-Induced Breakdown Spectroscopy—Applications for Production Control and Quality Assurance in the Steel Industry," *Spectrochimica Acta*, Pt. B, Vol. 56, 2001, pp. 637–649.

[14]Carranza, J. E., Fisher, B. T., Yoder, G. D., and Hahn, D. W., "On-line Analysis of Ambient Air Aerosols Using Laser-Induced Breakdown Spectroscopy," *Spectrochimica Acta, Part B*, Vol. 56, 2001, pp. 851–864.

[15]Zhang, H., Yueh, F. Y., and Singh, J. P., "Laser Induced Breakdown Spectrometry as a Multimetal Continuous Emission Monitor," *Applied Optics*, Vol. 38, No. 9, 1999, pp. 1459–1466.

[16]Ottesen, D. K., Wang, J. C. F., and Radziemski, L. J., "Real-Time Laser Spark Spectroscopy of Particulates in Combustion Environments," *Applied Spectroscopy.*, Vol. 43, No. 6, 1987, pp. 967–976.

[17]Zhang, H., Singh, J. P., Yueh, F. Y., and Cook, R. L., "Laser Induced Breakdown Spectra in a Coal-Fired MHD Facility," *Applied Spectroscopy*, Vol. 49, No. 11, 1995, pp. 1617–1623.

[18]Zhang, H., Yueh, F. Y., Singh, J. P., Cook, R. L., and Loge, G. W., "Laser Induced Breakdown Spectroscopy in Metal Seeded Flame," AIAA Paper 2000-2907, July 2000.

[19]Martin, G. A., Fuhr, J. R., and Wiese, W. L., "Atomic Transition Probabilities, Scandium Through Manganese," *Journal of Physical Chemistry*, Ref. Data 17, Supplement No. 3, 1988.

[20]Fuhr, J. R., Martin, G. A., and Wiese, W. L., "Atomic Transition Probabilities, Iron Through Nickel," *Journal of Physical Chemistry*, Ref. Data 17, Supplement No. 4, 1988.

[21]Cheskis, S., Derzy, I., Lozovsky, V. A., Kachanov, A., and Romanini, D., "Cavity Ring-Down Spectroscopy of OH Radicals in Low Pressure Flame," *Applied Physics*, Vol. B66, No. 3, 1998, pp. 377–381.

[22]Lozovsky, V. A., Derzy, I., and Cheskis, S., "Non Equilibrium Concentrations of the Vibrationally Excited OH Radical in a Methane Flame Measured by Cavity Ring-Down Spectroscopy," *Chemical Physics Letter*, Vol. 284, No. 5–6, 1998, pp. 407–411.

[23]Cheskis, S., "Quantitative Measurements of Absolute Concentrations of Intermediate Species in Flames," *Progress in Energy and Combustion Science*, Vol. 25, No. 3, 1999, pp. 233–252.

[24]Luque, J., and Crosley, D. R., "LIFBASE: Database and Spectral Simulation Program," SRI International, SRI Rept. MP 99-009, Menlo Park, CA, 1999.

R. P. Lucht
Associate Editor